

## Coevolutionary dynamics on scale-free networks

Sungmin Lee and Yuxin Kim

Department of Physics and Research Institute for Basic Sciences, Kyung Hee University, Seoul 130-701, Korea

We investigate Bak-Sneppen coevolution models on scale-free networks with various degree exponents including random networks. For  $\gamma > 3$ , the critical fitness value  $f_c$  approaches to a nonzero finite value in the limit  $N \rightarrow \infty$ , whereas  $f_c$  approaches to zero as  $2 < \gamma < 3$ . These results are explained by showing analytically  $f_c(N) \propto A = \langle (k+1)^2 \rangle_N^{\text{const}}$  on the networks with size  $N$ . The avalanche size distribution  $P(s)$  shows the normal power-law behavior for  $\gamma > 3$ . In contrast,  $P(s)$  for  $2 < \gamma < 3$  has two power-law regimes. One is a short regime for small  $s$  with a large exponent  $\gamma_1$  and the other is a long regime for large  $s$  with a small exponent  $\gamma_2$  ( $\gamma_1 > \gamma_2$ ). The origin of the two power-regimes is explained by the dynamics on an artificially-made star-linked network.

PACS numbers: 87.10.+e, 05.40.-a, 87.23.-n

Bak and Sneppen (BS) [1] has introduced an excellent model to explain the evolution of bio-species which exhibits the punctuated equilibrium behavior [2]. BS model has two important features, coevolution of the interacting species and the intermittent bursts of activity separating relatively long periods of the stasis. In BS model the ecosystem evolves into a self-organized criticality with avalanches of mutations occurring all scales. A side from its importance for the evolution BS model has been also shown to have rich scaling behaviors [3].

Since BS model was suggested, the model has been extensively studied on regular lattices or networks [3]. However, many important bio-systems have been elucidated to form nontrivial networks by the recently developed network theories [4]. Important examples are metabolic network, cellular network, and protein network [5, 6, 7, 8]. Especially the important bio-networks are scale-free networks (SFNs) [4], in which the degree distribution  $p(k)$  satisfies a power law  $p(k) \propto k^{-\gamma}$  [4]. Thus it is important to study the BS dynamics on SFNs or to find out how the base structure of interacting biological elements (cells, proteins, or species) affects the evolutionary change or dynamics of the given bio-system. Until now BS models on the nontrivial networks were not investigated extensively. Christensen et al. [9] have studied BS model on random networks (RNs). Kulkani et al. [11] studied BS model on small-world networks. Slanina and Kotrla [12] studied the forward avalanches of a sort of extremal dynamics with evolving networks. Moreno and Vazquez [13] studied BS model only on a SFN with  $\gamma = 3$ .

In this letter, we will study BS models on SFNs in complete and comprehensive ways. One of the main purposes of this study is to find which structure of interacting species is the most stable network or most close to mutation-free network under the coevolutionary change with interacting species. As is well-known, SFN with the degree exponent  $2 < \gamma < 3$  are physically much different from those with  $\gamma > 3$  [4]. We study BS models not only

on SFNs with  $2 < \gamma < 3$  but also on SFNs with  $\gamma > 3$  including random networks (or SFN with  $\gamma = 1$ ). As we shall see, two important results are found in this study. First, the critical fitness value  $f_c$  of BS models for  $\gamma > 3$  is shown to have the limiting behavior  $f_c(N) \rightarrow 0$  when the number of nodes  $N$  of the network goes to infinity. In contrast,  $f_c$  approaches a finite nonzero value as  $N \rightarrow \infty$  for  $2 < \gamma < 3$ . Furthermore,  $f_c(N)$  on SFNs with finite  $N$  is shown to satisfy the relation  $f_c(N) \propto \frac{\text{const.}}{\langle (k+1)^2 \rangle_N^{\text{const.}}}$ , which is also directly supported by simulation. Second, for  $2 < \gamma < 3$  the distribution of avalanches is shown to have two power-law regimes. To find the origin of this anomalous behavior of avalanches we also study BS models on an artificially-made star-linked network and find the similar two power-law regimes.

We now explain the model treated in this letter. All the models are defined on a graph  $G = fN; K g$ , where  $N$  is the number of nodes and  $K$  is the number of degrees with the average degree  $\langle k \rangle = 2K/N$ . Initially, a random fitness value  $f_i \in [0; 1]$  is assigned to each node  $i = 1, \dots, N$ . At each time step, the system is updated by the following two rules: (I) first assign new fitness value to the node with the smallest fitness value  $f_{\text{min}}$ . (II) Second assign new fitness values to the nodes which are directly connected to the node with  $f_{\text{min}}$ . We use SFNs with the various degree exponent as  $G = fN; K g$ . To generate SFNs, we use the static model [14] instead of preferential attachment algorithm [4].

To understand the dependence of the critical fitness value  $f_c(N)$  on  $N$ , we generate SFNs with  $\gamma = 1, 2, 3, 4, 5, 6, 7, 8$ . To exclude the effects of finite percolation clusters [9] and to see the effect of network structure itself, all the networks are made to have average degree  $\langle k \rangle = 4$ . To understand the dependence on number of nodes  $N$ , the networks with the sizes  $N = 10^3, \dots, 10^6$  are generated for each  $\gamma$ . To determine the critical fitness value  $f_c(N)$ , we consider  $f_{\text{min}}$  as a function of the total number of updates  $s$  [3]. Initially,  $f_{\text{min}}(s=0)$  is the gap  $G(0)$ , where  $G(s)$  is the maximum of all  $f_{\text{min}}(s')$  for  $0 \leq s' \leq s$  [3]. When  $G(s)$  jumps to a new higher value, there are no nodes in the system with  $f_i(s) < G(s)$ . Thus  $\lim_{s \rightarrow \infty} G_N(s) = f_c(N)$ .

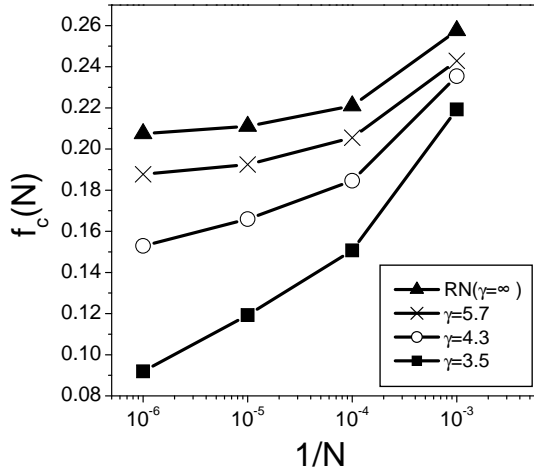


FIG. 1: Semilog plot of the threshold  $f_c(N)$  versus  $1/N$  on RN and on SFNs with  $\gamma = 5.7, 4.3$ , and  $3.5$ . Used networks sizes for each network are  $N = 10^3, 10^4, 10^5$ , and  $10^6$ . The solid lines between data points are obtained by simple linear interpolations.

Measure  $f_c(N)$  on the various SFNs. Fig. 1 shows the plot of  $f_c(N)$  versus  $1/N$  for SFNs with various  $\gamma$ . The values of critical fitness  $f_c(N \rightarrow 1)$  evaluated from data in Fig. 1 are  $0.21(1)$ ,  $0.19(1)$ ,  $0.15(1)$ , and  $0.09(1)$  for  $\gamma = 1, 5.7, 4.3$ , and  $3.5$ . The results in Fig. 1 mean that for  $\gamma > 3$ ,  $f_c(N \rightarrow 1) \rightarrow \text{const} > 0$ .

Fig. 2 shows the plot of  $f_c(N)$  versus  $1/N$  for  $2 < \gamma < 3$ . For  $\gamma = 3$ ,  $f_c(N)$  nicely satisfies the relation,  $f_c(N) = 1/\ln N$  [13]. For  $2 < \gamma < 3$ ,  $f_c(N)$ 's seem to follow a power-law  $f_c(N) \sim N^{-\gamma}$  and approach to zero as  $N$  goes to 1. In contrast to the results in Fig. 1,  $f_c \neq 0$  for  $2 < \gamma < 3$ .

In the RN, every pair of nodes are randomly connected and the degree distribution is a Poisson distribution [4, 9]. So the BS model on RN [9] is a good realization of the mean-field-type random neighbor model. In the random neighbor model, the fitness values of the randomly selected ( $m = 1$ ) nodes as well as the node with  $f_{m \text{ in}}$  are updated and  $f_c = 1/m$  [10]. The result  $f_c(1) = 0.21(1)$  on RN is very close to  $\frac{1}{\langle k \rangle + 1} = \frac{1}{5}$ , which is expected one from the random neighbor model by setting  $\langle k \rangle + 1 = m$  [9]. In the steady state of BS model, the probability measure  $P(f < f_c)$  is 0. Suppose the case that the number of updates for each step is fixed as  $m$ , as in the random neighbor model. To sustain the steady state in the case, at most one new fitness value should be less than  $f_c$  and the other  $m - 1$  new values should be larger than  $f_c$  [10]. Therefore we can easily see  $m f_c = 1$  or  $f_c = 1/m$ .

On a network the number of updates depends on the degree of the node with  $f_{m \text{ in}}$  and the probability which a node with degree  $k$  is connected to the node with  $f_{m \text{ in}}$  should be proportional to  $k$ . For an updating step the probability that a node with degree  $k$  is updated is proportional to  $k + 1$ , because the node itself can be the

node with  $f_{m \text{ in}}$ . Therefore, after an arbitrary update, the probability  $P_{m \text{ in}}(k)$  of a node with degree  $k$  being the node with  $f_{m \text{ in}}$  is proportional to  $k + 1$ . This means that  $P_{m \text{ in}}(k)$  in the steady state should be proportional to  $k + 1$ , or  $P_{m \text{ in}}(k) = \frac{P(k+1)p(k)}{k(k+1)p(k)} = \frac{1}{\langle k \rangle + 1} (k+1)p(k)$ . The average number  $N_{\text{update}}$  of the nodes updated for one updating process is therefore

$$N_{\text{update}} = \frac{X}{(k+1)P_{m \text{ in}}(k)} = \frac{P}{k} \frac{(k+1)^2 p(k)}{\langle k \rangle + 1} \quad (1)$$

and thus  $f_c$  is

$$f_c = \frac{1}{N_{\text{update}}} = \frac{P}{k} \frac{\langle k \rangle + 1}{(k+1)^2 p(k)} = \frac{\langle k \rangle + 1}{\langle (k+1)^2 \rangle} : \quad (2)$$

When the number of updates is fixed as  $m$ , Eq. (2) reproduces the mean-field result  $f_c = 1/m$ . In SFNs with  $p(k) \propto k^{-\gamma}$ , Eq. (2) becomes

$$f_c \sim \frac{1}{\frac{A}{\langle k^2 \rangle}} = \frac{A}{\frac{A}{k^2} dk} ; \begin{cases} > 3 & \\ 2 < \gamma < 3 & \end{cases} \quad (3)$$

Eq. (3) explains the results in Figs. 1 and 2 including the result  $f_c \sim \frac{1}{\ln N}$  for  $\gamma = 3$ . For  $2 < \gamma < 3$ , measured  $f_c(N)$  is fitted to the relation  $f_c(N) = A = \langle k^2 \rangle_N^{-1}$ , where  $A$  is constant and  $\langle k^2 \rangle_N$  is  $\langle k^2 \rangle$  for the network with the size  $N$ . The fitted lines in Fig. 2 show that the relation  $f_c(N) = A = \langle k^2 \rangle_N^{-1}$  holds well and directly supports Eq. (3).

An avalanche in Bak-Sneppen model is defined as the sequential steps for which the minimal site has a fitness value smaller than given  $f_o$  [3]. For each network, we choose  $f_o$  to satisfy  $(f_c(N) - f_o) = f_c(N) = 0.05$ . The probability distribution  $P(s)$  of avalanche size  $s$  on the

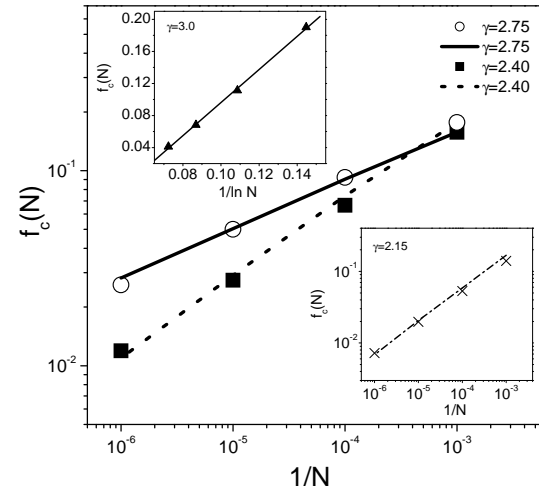


FIG. 2: Log-log plot of  $f_c(N)$  and  $A = \langle k(N)^2 \rangle_N$  versus  $1/N$  on SFNs with  $\gamma = 2.75, 2.40$ , and  $2.15$ . Symbols are for  $f_c(N)$  and the lines are for  $A = \langle k(N)^2 \rangle_N$ , where  $A$  is a constant. The top inset shows the plot of  $f_c(N)$  versus  $1 = \ln N$  for  $\gamma = 3.0$ .

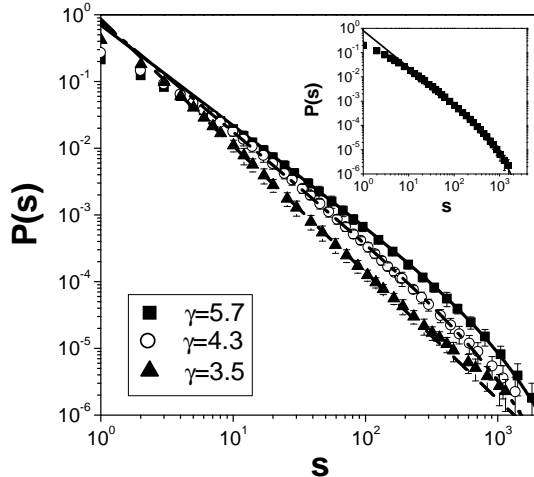


FIG. 3: Log-log plot of the avalanche size distribution  $P(s)$  on SFNs with  $\gamma = 5.7$ ,  $\gamma = 4.3$ ,  $\gamma = 3.5$  and on RN (Inset). The curves for  $\gamma = 5.7$ ,  $\gamma = 4.3$  and RN denote the fits of the form  $P(s) = As^{-\gamma} \exp(-s/s_c)$  to the data. Obtained exponents are  $\gamma = 1.5$  for both  $\gamma = 5.7$  and RN, and  $\gamma = 1.65$  for  $\gamma = 4.3$ . The line for  $\gamma = 3.5$  denotes the fit of the form  $P(s) = As^{-\gamma}$  ( $\gamma = 1.65$ ) without cut-off.

networks with the size  $N = 10^6$  are shown in Fig. 3 and Fig. 4. All the data in Figs. 3 and 4 are taken in the steady-states.

As is shown in Fig. 3,  $P(s)$  in SFNs with  $\gamma > 3$  including RN satisfy the normal power-law behavior with an exponential cut-off as  $P(s) = As^{-\gamma} \exp(-s/s_c)$ . The curves in Fig. 3 represent the fitted curves to data for  $P(s)$ . From those fittings the obtained values for  $\gamma$  are 1.5 for RN and  $\gamma = 5.7$ , and 1.65 for  $\gamma = 4.3$ . The result for RN and SFN with  $\gamma = 5.7$  is expected from the random neighbor model [10]. As  $\gamma$  decreases to 4.0 or so increases to 1.65. For  $\gamma = 3.5$ , however, the best fitting function is  $P(s) = Bs^{-\gamma}$  with  $\gamma = 1.65$  and we cannot find the cut-off-dependent behavior within our data. Instead, it is even observed that tails of measured data for  $\gamma = 3.5$  around  $s = 10^3$  seem to deviate from the fitting function  $P(s) = Bs^{-\gamma}$  and are larger than values estimated from the best fitting function. This rather anomalous tail behavior of  $P(s)$  for  $\gamma = 3.5$  should be the signal of the anomalous behavior of  $P(s)$  for  $2 < \gamma < 3$ .

In contrast to the simple power-law behavior for  $\gamma > 3$ , anomalous behavior for  $P(s)$  shows up for  $2 < \gamma < 3$  (Fig. 4). We can see two power-law regimes clearly for  $P(s)$  in Fig. 4. Initially the avalanche size distribution follows  $P(s) \propto s^{-\gamma_1}$  about 1 decade or so. After this short initial power-law regime, the long second power-law regime appears as  $P(s) \propto s^{-\gamma_2}$ , where  $\gamma_1 > \gamma_2$ . The measured exponents  $\gamma_1$ ,  $\gamma_2$  are summarized in Table I.

Compared to the behavior of the avalanche size distribution for  $\gamma > 3$ , this anomalous behavior of  $P(s)$  is very peculiar. In the steady state, it is expected that the node with  $f_m$  (the minimal node) is most frequently found among the last updated nodes [10] and then the

TABLE I: Two power-law exponents,  $\gamma_1$  and  $\gamma_2$  for SFNs with  $\gamma < 3$ .

	$\gamma_1$	$\gamma_2$
3.0	2.09	1.59
2.75	2.22	1.47
2.4	2.27	1.32
2.15	2.30	1.20

mininal node locally performs a random walk. However, there can be longer jumps of any length with a very low probability. If this kind of a jumping random walk is the motion of the minimal node, then a subnetwork consists of a hub node (center node) and many slave nodes directly linked to the hub should be important to decide the behavior of  $P(s)$ . Due to the jumping random walk behavior, the more slave nodes the hub node has, the longer stay of the minimal node or the longer avalanche exists at the given subnetwork. This effect explains the second power-law regime with the exponent  $\gamma_2$  in Fig. 4, because  $\langle k^2 \rangle$  diverges for  $2 < \gamma < 3$ , and so the subnetwork of a hub node and many slave nodes should be the main substructure in SFNs with  $2 < \gamma < 3$ . Evidently, the jumping steps of the jumping random walk make the shorter avalanches possible and this effect explains the first power-law regime with the exponent  $\gamma_1$ .

To support the qualitative explanation of the two power-law regimes, we consider an artificially-made star-linked network shown in Fig. 5. In the star-linked network, a main subnetwork consists of a center (star) node and many dangling slave nodes linked directly to the star node. Then the center nodes are linked hierarchically to one after another as sketched in Fig. 5(a). We make a star-linked network in which there are 25 base sub-

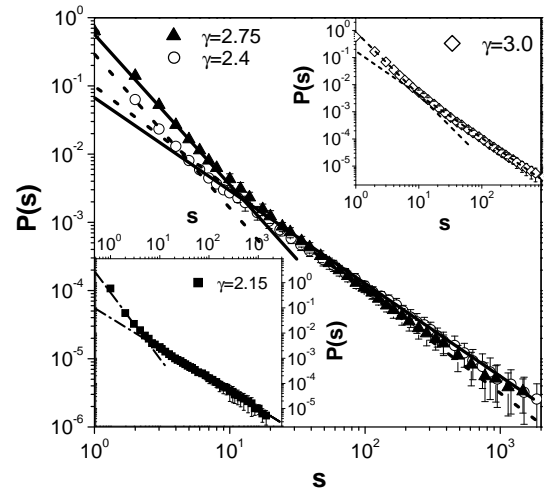


FIG. 4: Log-log plot of  $P(s)$  on SFNs with  $\gamma = 3$  (top inset), 2.75, 2.4, and 2.15. Two crossing lines for each data sets denote the two power-law regimes,  $P(s) = As^{-\gamma_1}$  and  $P(s) = Bs^{-\gamma_2}$ . Obtained exponents,  $\gamma_1$  and  $\gamma_2$ , are shown in Table I.

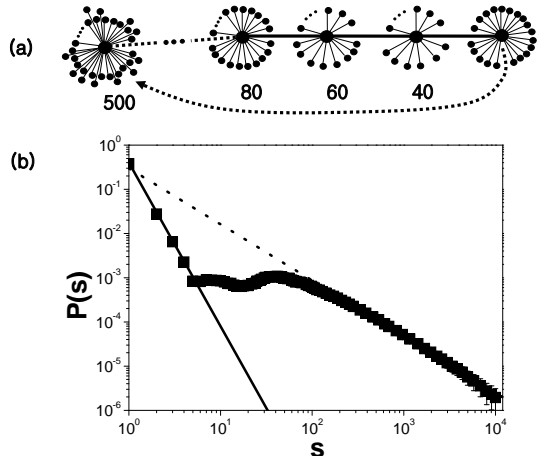


FIG. 5: (a) Schematic diagram of a star-linked network which consists of 25 subnetworks with 500, 480, ..., and 20 dangling slave nodes. (b) Plot of  $P(s)$  on the star-linked network structure. Two power-law regimes with  $P(s) = A s^{-\gamma_1}$  ( $\gamma_1 = 3.7$ ) and  $P(s) = B s^{-\gamma_2}$  ( $\gamma_2 = 1.27$ ) are clearly shown by the lines.

networks with 500, 480, ..., and 20 slave nodes, respectively. In this network, we perform BS dynamics and  $f_c = 0.123$ .  $P(s)$  is also measured on the star-linked network and is shown in Fig. 5(b). We find the very two power-law regimes with the exponents  $\gamma_1 = 3.7$  and  $\gamma_2 = 1.27$ . The plateau between two power-regimes in the data of  $P(s)$  in Fig. 5(b) is probably from the discrete distribution of the number of slave nodes.

In conclusion, we study BS models on SFNs with various  $\gamma$ . For  $\gamma > 3$ ,  $f_c$  approaches to a nonzero value in the limit  $N \rightarrow \infty$  and  $P(s)$  shows normal power-law behavior with  $\gamma = 1.5$ . For  $\gamma < 3$ ,  $f_c$  approaches to zero as  $f_c(N) \sim 1/N$  and  $P(s)$  has two power-law regimes. The origin of the two power-regimes are explained by the dynamics on a star-linked network.

In Ref. [13], BS dynamics only on a SFN with  $\gamma = 3$  was studied and the only meaningful numerical result was to show  $f_c(N) \sim 1/\ln N$ . Ref. [13] suggested a relation similar to Eq. (2) from a rate equation which was obtained by a naive and immature analogy of BS dy-

namics to the epidemic dynamics on SFNs [15]. However the rate equation should never be the exact one. Even the exact rate equation for the simple random neighbor model [10] is much more complex than that of Ref. [13] or the epidemic dynamics. The correct rate equation for BS dynamics on SFNs must be derived by considering all the terms of the rate equation in Ref. [10] and the base network structure simultaneously and correctly. The derivation of the correct rate equation should be a subject for the future study. In Ref. [13] they argued  $P(s)$  for  $\gamma = 3$  satisfies a simple power-law with  $\gamma = 1.55$ . By the brute-force fit of the relation  $P(s) \sim s^{-\gamma}$  to our data in Fig. 4, we also obtain  $\gamma = 1.6$  for  $\gamma = 3$ . However, this blind application of the simple power law should be wrong and there should exist the two power-law regimes even for  $\gamma = 3$ . One can easily identify the two power-law regimes in the  $P(s)$  data of Ref. [13] rather clearly although the tail parts of their data are qualitatively poor and show large fluctuations.

The occurrence of two power-law regimes for  $P(s)$  was also found in BS dynamics on small-world networks [11] and in an extremal dynamics with evolving networks [12]. However the origins of the two power-law regimes were completely different from ours. The origin in the small-world networks was argued to be the long range connectivity of the networks [11]. The extremal dynamics with evolving random networks [12] changes the network structure and is not exactly the same as BS dynamics. Furthermore the evolving network develops many disconnected clusters. In the model [12] the forward avalanches are mainly measured. The forward avalanches [12] should be affected by the dynamical aggregate and splitting of subnetworks by the extremal dynamics, which should be the origin of the two power-law regimes. In contrast our avalanches of BS dynamics is measured on a fully-connected static scale-free network and should not be directly comparable to the avalanches on dynamically varying networks.

Authors would like to thank Prof. H. Jeong for valuable suggestions. This work is supported by Korea Research Foundation Grant No. KRF-2004-015-C 00185.

- 
- [1] P. Bak and K. Sneppen, *Phys. Rev. Lett.* **71**, 4083 (1993).  
 [2] S. A. Kauffman and S. J. Johnsen, *Theoretical Biology* **149**, 467 (1991).  
 [3] M. Paczuski, S. Maslov and P. Bak, *Phys. Rev. E* **53**, 414 (1996).  
 [4] R. Albert and A.-L. Barabasi, *Rev. Mod. Phys.* **74**, 47 (2002); S. N. Dorogovtsev and J. F. F. Mendes, *Adv. Phys.* **51**, 1079 (2002).  
 [5] H. Jeong, B. Tomber, R. Albert, Z. N. Oltvai and A.-L. Barabasi, *Nature (London)* **407**, 651 (2000).  
 [6] H. Jeong, S. Mason, A.-L. Barabasi and Z. N. Oltvai, *Nature (London)* **411**, 41 (2001).  
 [7] R. J. Williams and N. D. Martinez, *Nature (London)* **404**, 180 (2000).  
 [8] J. C. Amado, R. Guimera and L. A. N. Amaral, *Phys. Rev. E* **65**, 030901(R) (2002).  
 [9] K. Christensen, R. Donangelo, B. Kaoller and K. Sneppen, *Phys. Rev. Lett.* **81**, 2380 (1998).  
 [10] H. Flyvbjerg, K. Sneppen, and P. Bak, *Phys. Rev. Lett.* **71**, 4087 (1993).  
 [11] R. V. Kulkarni, E. Almås and D. Stroud, cond-mat/9905066.  
 [12] F. Slanina and M. Kotrla, *Phys. Rev. Lett.* **83**, 5587 (1999); *Phys. Rev. E* **62**, 6170 (2000).  
 [13] Y. Moreno and A. Vazquez, *Europhys. Lett.* **57**, 765 (2002).

- [14] K.-I. Goh, B. Kahng and D. Kim, Phys. Rev. Lett. 87, 278701 (2001).  
[15] R. Pastor-Satorras and A. Vespignani, Phys. Rev. Lett. 86, 3200 (2001); Phys. Rev. E. 63, 066117 (2001).